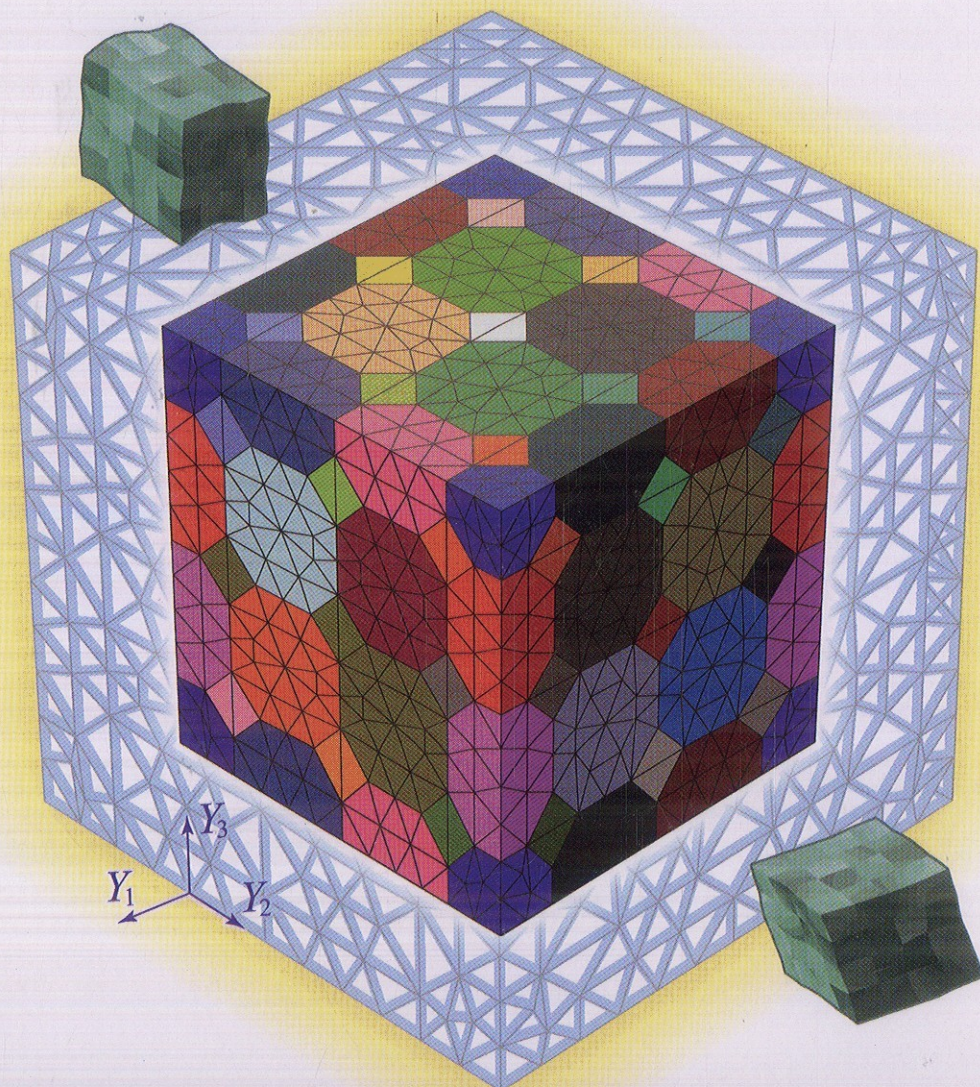


Miguel Vaz Jr., Eduardo A. de Souza  
Neto and Pablo A. Muñoz-Rojas (Eds.)

WILEY-VCH

# Advanced Computational Materials Modeling

From Classical to Multi-Scale Techniques



# Contents

**Preface** *XIII*

**List of Contributors** *XV*

## **1 Materials Modeling – Challenges and Perspectives** *1*

*Miguel Vaz Jr., Eduardo A. de Souza Neto, and Pablo Andres Muñoz-Rojas*

### **1.1 Introduction** *1*

### **1.2 Modeling Challenges and Perspectives** *3*

#### **1.2.1 Mechanical Degradation and Failure of Ductile Materials** *3*

##### **1.2.1.1 Remarks** *7*

##### **1.2.2 Modeling of Cellular Structures** *8*

##### **1.2.2.1 Remarks** *14*

##### **1.2.3 Multiscale Constitutive Modeling** *15*

##### **1.3 Concluding Remarks** *18*

Acknowledgments *19*

References *19*

## **2 Local and Nonlocal Modeling of Ductile Damage** *23*

*José Manuel de Almeida César de Sá, Francisco Manuel Andrade Pires,  
and Filipe Xavier Costa Andrade*

### **2.1 Introduction** *23*

### **2.2 Continuum Damage Mechanics** *25*

#### **2.2.1 Basic Concepts of CDM** *25*

#### **2.2.2 Ductile Plastic Damage** *26*

#### **2.3 Lemaitre's Ductile Damage Model** *27*

##### **2.3.1 Original Model** *27*

##### **2.3.1.1 The Elastic State Potential** *28*

##### **2.3.1.2 The Plastic State Potential** *29*

##### **2.3.1.3 The Dissipation Potential** *29*

##### **2.3.1.4 Evolution of Internal Variables** *30*

##### **2.3.2 Principle of Maximum Inelastic Dissipation** *31*

##### **2.3.3 Assumptions Behind Lemaitre's Model** *32*

#### **2.4 Modified Local Damage Models** *33*

#### **2.4.1 Lemaitre's Simplified Damage Model** *33*

2.4.1.1	Constitutive Model	33
2.4.1.2	Numerical Implementation	34
2.4.2	Damage Model with Crack Closure Effect	37
2.4.2.1	Constitutive Model	37
2.4.2.2	Numerical Implementation	40
2.5	Nonlocal Formulations	42
2.5.1	Aspects of Nonlocal Averaging	44
2.5.1.1	The Averaging Operator	44
2.5.1.2	<i>Weight Functions</i>	45
2.5.2	Classical Nonlocal Models of Integral Type	45
2.5.2.1	Nonlocal Formulations for Lemaitre's Simplified Model	46
2.5.3	Numerical Implementation of Nonlocal Integral Models	47
2.5.3.1	Numerical Evaluation of the Averaging Integral	48
2.5.3.2	Global Version of the Elastic Predictor/Return Mapping Algorithm	49
2.6	Numerical Analysis	57
2.6.1	Axisymmetric Analysis of a Notched Specimen	57
2.6.2	Flat Grooved Plate in Plane Strain	62
2.6.3	Upsetting of a Tapered Specimen	63
2.6.3.1	Damage Prediction Using the Lemaitre's Simplified Model	65
2.6.3.2	Damage Prediction Using the Lemaitre's Model with Crack Closure Effect	67
2.7	Concluding Remarks	68
	Acknowledgments	69
	References	69

### **3 Recent Advances in the Prediction of the Thermal Properties of Metallic Hollow Sphere Structures 73**

*Thomas Fiedler, Irina V. Belova, Graeme E. Murch, and Andreas Öchsner*

3.1	Introduction	73
3.2	Methodology	74
3.2.1	Lattice Monte Carlo Method	75
3.2.2	Finite Element Method	77
3.2.2.1	Basics of Heat Transfer	77
3.2.2.2	Weighted Residual Method	77
3.2.2.3	<i>Discretization and Principal Finite Element Equation</i>	78
3.2.3	Numerical Calculation Models	89
3.3	Finite Element Analysis on Regular Structures	91
3.4	Finite Element Analysis on Cubic-Symmetric Models	94
3.5	LMC Analysis of Models of Cross Sections	98
3.5.1	Modeling	98
3.5.2	Results	101
3.6	Computed Tomography Reconstructions	103
3.6.1	Computed Tomography	104
3.6.2	Numerical Analysis	104
3.6.2.1	Microstructure	105

3.6.2.2	Mesostructure	106
3.6.3	Results	106
3.7	Conclusions	108
	References	109
<b>4</b>	<b>Computational Homogenization for Localization and Damage</b>	<b>111</b>
	<i>Thierry J. Massart, Varvara Kouznetsova, Ron H. J. Peerlings, and Marc G. D. Geers</i>	
4.1	Introduction	111
4.1.1	Mechanics Across the Scales	111
4.1.2	Some Historical Notes on Homogenization	112
4.1.3	Separation of Scales	113
4.1.4	Computational Homogenization and Its Application to Damage and Fracture	114
4.2	Continuous–Continuous Scale Transitions	115
4.2.1	First-Order Computational Homogenization	115
4.2.2	Second-Order Computational Homogenization	119
4.2.3	Application of the Continuous–Continuous Homogenization Schemes to Ductile Damage	121
4.3	Continuous–Discontinuous Scale Transitions	125
4.3.1	Scale Transitions and RVE for Initially Periodic Materials	126
4.3.1.1	First-Order Scale Transitions	126
4.3.1.2	Choice of the Mesoscopic Representative Volume Element	127
4.3.1.3	Boundary Conditions for the Unit Cell	128
4.3.2	Localization of Damage at the Fine and Coarse Scales	129
4.3.2.1	Fine-Scale Localization – Implicit Gradient Damage	129
4.3.2.2	Detection of Coarse-Scale Localization as a Bifurcation into an Inhomogeneous Deformation Pattern	130
4.3.2.3	Illustration of the Localization Analysis	132
4.3.2.4	Identification and Selection of the Localization Orientation	135
4.3.3	Localization Band Enhanced Multiscale Solution Scheme	135
4.3.3.1	Introduction of the Localization Band	136
4.3.3.2	Coupled Multiscale Scheme for Localization	137
4.3.4	Scale Transition Procedure for Localized Behavior	139
4.3.4.1	Multiscale Solution Procedure	139
4.3.4.2	Causes of Snapback in the Averaged Material Response	139
4.3.4.3	Strain Jump Control for Embedded Band Snapback	140
4.3.4.4	Dissipation Control for Unit-Cell Snapback	141
4.3.5	Solution Strategy and Computational Aspects	142
4.3.5.1	Governing Equations for the Macroscopic and Mesoscopic Solution Procedures	142
4.3.5.2	Extraction of Consistent Tangent Stiffness for Unit-Cell Snapback Control	144
4.3.5.3	Discretization and Linearization of the Macroscopic Solution Procedure	144

4.3.5.4	Introduction of Localization Bands upon Material Bifurcation	146
4.3.6	Applications and Discussion	147
4.3.6.1	Selection of Localized Solutions	147
4.3.6.2	Mesostructural Snapback in a Tension–Compression Test	149
4.3.6.3	Size Effect in a Shear–Compression Test	151
4.3.6.4	Masonry Shear Wall Test	152
4.4	Closing Remarks	159
	References	160
<b>5</b>	<b>A Mixed Optimization Approach for Parameter Identification Applied to the Gurson Damage Model</b>	<b>165</b>
	<i>Pablo Andres Muñoz-Rojas, Luiz Antonio B. da Cunha, Eduardo L. Cardoso, Miguel Vaz Jr., and Guillermo Juan Creus</i>	
5.1	Introduction	165
5.2	Gurson Damage Model	166
5.2.1	Influence of the Parameter Values on Behavior of the Damage Model	171
5.2.2	Recent Developments and New Trends in the Gurson Model	175
5.3	Parameter Identification	177
5.4	Optimization Methods – Genetic Algorithms and Mathematical Programming	179
5.4.1	Genetic Algorithms	180
5.4.1.1	Formulation	181
5.4.1.2	Implementation	184
5.4.2	Gradient-Based Methods	184
5.4.2.1	General Procedure	184
5.4.2.2	Sequential Linear Programming (SLP)	185
5.4.2.3	Globally Convergent Method of Moving Asymptotes (GCMMA)	185
5.5	Sensitivity Analysis	187
5.5.1	Modified Finite Differences and the Semianalytical Method	188
5.6	A Mixed Optimization Approach	192
5.7	Examples of Application	192
5.7.1	Low Carbon Steel at 25 °C	192
5.7.2	Aluminum Alloy at 400 °C	197
5.8	Concluding Remarks	200
	Acknowledgments	200
	References	201
<b>6</b>	<b>Semisolid Metallic Alloys Constitutive Modeling for the Simulation of Thixoforming Processes</b>	<b>205</b>
	<i>Roxane Koeune and Jean-Philippe Ponthot</i>	
6.1	Introduction	205
6.2	Semisolid Metallic Alloys Forming Processes	207
6.2.1	Thixotropic Semisolid Metallic Alloys	208
6.2.2	Different Types of Semisolid Processing	209

6.2.2.1	Production of Spheroidal Microstructure	210
6.2.2.2	Reheating	212
6.2.2.3	Forming	213
6.2.3	Advantages and Disadvantages of Semisolid Processing	215
6.3	Rheological Aspects	216
6.3.1	Microscopic Point of View	216
6.3.1.1	Origins of Thixotropy	216
6.3.1.2	Transient Behavior	217
6.3.1.3	Effective Liquid Fraction	222
6.3.2	Macroscopic Point of View	222
6.3.2.1	Temperature Effects	222
6.3.2.2	Yield Stress	222
6.3.2.3	Macrosegregation	223
6.4	Numerical Background in Large Deformations	223
6.4.1	Kinematics in Large Deformations	223
6.4.1.1	Lagrangian Versus Eulerian Coordinate Systems	223
6.4.1.2	Deformation Gradient and Strain Rate Tensors	225
6.4.2	Finite Deformation Constitutive Theory	225
6.4.2.1	Principle of Objectivity	225
6.4.2.2	Different Classes of Materials	226
6.4.2.3	A Corotational Formulation	228
6.4.2.4	Linear Elastic Solid Material Model	229
6.4.2.5	Linear Newtonian Liquid Material Model	230
6.4.2.6	Hypoelastic Solid Material Models	231
6.4.2.7	Liquid Material Models	236
6.4.2.8	Comparison of Solid and Liquid Approaches	236
6.5	State-of-the-Art in FE-Modeling of Thixotropy	237
6.5.1	One-Phase Models	237
6.5.1.1	Apparent Viscosity Evolution	238
6.5.1.2	Yield Stress Evolution	243
6.5.2	Two-Phase Models	244
6.5.2.1	Two Coupled Fields	244
6.5.2.2	Coupling Sources	245
6.6	A Detailed One-Phase Model	246
6.6.1	Cohesion Degree	247
6.6.2	Liquid Fraction	248
6.6.3	Viscosity Law	248
6.6.4	Yield Stress and Isotropic Hardening	250
6.7	Numerical Applications	250
6.7.1	Test Description	250
6.7.2	Results Analysis	251
6.7.2.1	First Validation of the Model under Isothermal Conditions	251
6.7.2.2	Thermomechanical Analysis	252
6.7.2.3	Residual Stresses Analysis	253
6.7.2.4	Internal Variables Analysis	253

6.8	Conclusion	254
	References	255
<b>7</b>	<b>Modeling of Powder Forming Processes; Application of a Three-invariant Cap Plasticity and an Enriched Arbitrary Lagrangian–Eulerian FE Method</b>	<b>257</b>
	<i>Amir R. Khoei</i>	
7.1	Introduction	257
7.2	Three-Invariant Cap Plasticity	260
7.2.1	Isotropic and Kinematic Material Functions	262
7.2.2	Computation of Powder Property Matrix	264
7.2.3	Model Assessment and Parameter Determination	265
7.2.3.1	Model Assessment	265
7.2.3.2	Parameter Determination	267
7.3	Arbitrary Lagrangian–Eulerian Formulation	269
7.3.1	ALE Governing Equations	270
7.3.2	Weak Form of ALE Equations	272
7.3.3	ALE Finite Element Discretization	273
7.3.4	Uncoupled ALE Solution	274
7.3.4.1	Material (Lagrangian) Phase	275
7.3.4.2	Smoothing Phase	276
7.3.4.3	Convection (Eulerian) Phase	278
7.3.5	Numerical Modeling of an Automotive Component	279
7.4	Enriched ALE Finite Element Method	282
7.4.1	The Extended-FEM Formulation	283
7.4.2	An Enriched ALE Finite Element Method	286
7.4.2.1	Level Set Update	287
7.4.2.2	Stress Update and Numerical Integration	288
7.4.3	Numerical Modeling of the Coining Test	291
7.5	Conclusion	295
	Acknowledgments	295
	References	296
<b>8</b>	<b>Functionally Graded Piezoelectric Material Systems – A Multiphysics Perspective</b>	<b>301</b>
	<i>Wilfredo Montealegre Rubio, Sandro Luis Vatanabe, Gláucio Hermogenes Paulino, and Emílio Carlos Nelli Silva</i>	
8.1	Introduction	301
8.2	Piezoelectricity	302
8.3	Functionally Graded Piezoelectric Materials	304
8.3.1	Functionally Graded Materials (FGMs)	304
8.3.2	FGM Concept Applied to Piezoelectric Materials	306
8.4	Finite Element Method for Piezoelectric Structures	309
8.4.1	The Variational Formulation for Piezoelectric Problems	309
8.4.2	The Finite Element Formulation for Piezoelectric Problems	310

8.4.3	Modeling Graded Piezoelectric Structures by Using the FEM	312
8.5	Influence of Property Scale in Piezotransducer Performance	314
8.5.1	Graded Piezotransducers in Ultrasonic Applications	314
8.5.2	Further Consideration of the Influence of Property Scale: Optimal Material Gradation Functions	319
8.6	Influence of Microscale	322
8.6.1	Performance Characteristics of Piezocomposite Materials	326
8.6.1.1	Low-Frequency Applications	326
8.6.1.2	High-Frequency Applications	328
8.6.2	Homogenization Method	328
8.6.3	Examples	332
8.7	Conclusion	335
	Acknowledgments	335
	References	336
<b>9</b>	<b>Variational Foundations of Large Strain Multiscale Solid Constitutive Models: Kinematical Formulation</b>	<i>341</i>
	<i>Eduardo A. de Souza Neto and Raúl A. Feijóo</i>	
9.1	Introduction	341
9.2	Large Strain Multiscale Constitutive Theory: Axiomatic Structure	343
9.2.1	Deformation Gradient Averaging and RVE Kinematics	346
9.2.1.1	Consequence: Minimum RVE Kinematical Constraints	346
9.2.1.2	Minimum Constraint on Displacement Fluctuations	347
9.2.2	Actual Constraints: Spaces of RVE Velocities and Virtual Displacements	348
9.2.3	Equilibrium of the RVE	349
9.2.3.1	Strong Form of Equilibrium	350
9.2.3.2	Solid–Void/Pore Interaction	350
9.2.4	Stress Averaging Relation	351
9.2.4.1	Macroscopic Stress in Terms of RVE Boundary Tractions and Body Forces	351
9.2.5	The Hill–Mandel Principle of Macrohomogeneity	352
9.3	The Multiscale Model Definition	353
9.3.1	The Microscopic Equilibrium Problem	354
9.3.2	The Multiscale Model: Well-Posed Equilibrium Problem	354
9.4	Specific Classes of Multiscale Models: The Choice of $\mathcal{V}_\mu$	356
9.4.1	Taylor Model	356
9.4.1.1	The Taylor-Based Constitutive Functional: the Rule of Mixtures	357
9.4.2	Linear RVE Boundary Displacement Model	359
9.4.3	Periodic Boundary Displacement Fluctuations Model	359
9.4.4	Minimum Kinematical Constraint: Uniform Boundary Traction	360
9.5	Models with Stress Averaging in the Deformed RVE Configuration	361
9.6	Problem Linearization: The Constitutive Tangent Operator	362
9.6.1	Homogenized Constitutive Functional	363
9.6.2	The Homogenized Tangent Constitutive Operator	364

9.7	Time-Discrete Multiscale Models	366
9.7.1	The Incremental Equilibrium Problem	367
9.7.2	The Homogenized Incremental Constitutive Function	367
9.7.3	Time-Discrete Homogenized Constitutive Tangent	368
9.7.3.1	Taylor Model	369
9.7.3.2	The General Case	369
9.8	The Infinitesimal Strain Theory	371
9.9	Concluding Remarks	372
	Appendix	373
	Acknowledgments	376
	References	376
10	<b>A Homogenization-Based Prediction Method of Macroscopic Yield Strength of Polycrystalline Metals Subjected to Cold-Working</b>	379
	<i>Kenjiro Terada, Ikumu Watanabe, Masayoshi Akiyama, Shigemitsu Kimura, and Kouichi Kuroda</i>	
10.1	Introduction	379
10.2	Two-Scale Modeling and Analysis Based on Homogenization Theory	382
10.2.1	Two-Scale Boundary Value Problem	383
10.2.2	Micro-Macro Coupling and Decoupling Schemes for the Two-Scale BVP	385
10.2.3	Method of Evaluating Macroscopic Yield Strength after Cold-Working	386
10.3	Numerical Specimens: Unit Cell Models with Crystal Plasticity	387
10.4	Approximate Macroscopic Constitutive Models	390
10.4.1	Definition of Macroscopic Yield Strength	391
10.4.2	Macroscopic Yield Strength at the Initial State	391
10.4.3	Approximate Macroscopic Constitutive Model	393
10.4.4	Parameter Identification for Approximate Macroscopic Constitutive Model	393
10.5	Macroscopic Yield Strength after Three-Step Plastic Forming	395
10.5.1	Forming Condition	395
10.5.2	Two-Scale Analyses with Micro-Macro Coupling and Decoupling Schemes	396
10.5.3	Evaluation of Macroscopic Yield Strength after Three-Step Plastic Forming	398
10.6	Application for Pilger Rolling of Steel Pipe	401
10.6.1	Forming Condition	401
10.6.2	Decoupled Microscale Analysis	403
10.6.3	Evaluation of Macroscopic Yield Strength after Pilger Rolling Process	406
10.7	Conclusion	408
	References	409
	<b>Index</b>	413